Br. J. Pharmacol. (1989), **98**, 1173–1184

Modulation of sodium current kinetics by chlorpromazine in freshly-isolated striatal neurones of the adult guinea-pig

Nobukuni Ogata & Hideharu Tatebayashi

Department of Pharmacology, Faculty of Medicine, Kyushu University, Fukuoka 812, Japan

1 The neurones of the striatum were freshly dissociated from the adult guinea-pig brain by enzymatic and mechanical treatments. Sodium channel current kinetics in these neurones were measured using a whole cell variation of the patch-clamp technique.

2 Chlorpromazine, a neuroleptic, in micromolar concentrations reversibly reduced the amplitude of the sodium currents. Activation and inactivation time constants were not affected. The inhibition followed one-to-one binding stoichiometry.

3 The concentration-response curve shifted to the left when the holding potential was less negative. The EC_{50} shifted from 4.8 μM to 0.9 μM when the holding potential was changed from -120 mV to -70 mV.

4 The steady-state activation curve of the sodium current was not affected by chlorpromazine, whereas the steady-state inactivation curve was shifted in the negative direction. Consequently, the window current which is normally present at a potential range around -50 mV was decreased in the presence of chlorpromazine.

5 Successive sodium currents evoked by a train of depolarizing pulses (30 ms duration) to -10 mV showed a cumulative decrease in size during the application of chlorpromazine. However, such 'use-dependent' block was not observed when the pulse duration was reduced to 1 ms.

6 The recovery from inactivation in the presence of chlorpromazine, was expressed as a second order process. The faster component was similar to the recovery time course of the normal sodium channels. The slower component accounted for the use-dependent effect of chlorpromazine.

7 The results indicate that chlorpromazine binds to the resting sodium channels producing steady-state block at a very negative holding potential. When the membrane is depolarized, chlorpromazine binds to the inactivated form of the sodium channels with much higher affinity and stabilizes them in the inactivated state, slowing their kinetics.

Introduction

The opening of the Na^+ channels is often blocked by various categories of chemical agents, and these agents have proved to be useful in understanding the physiology of channel gating (Narahashi, 1974). We have recently shown that micromolar concentrations of chlorpromazine (Cpz), a neuroleptic, blocks Na^+ channels in mouse cultured neuroblastoma cells (Ogata *et al.*, 1989b). A potent voltage-dependent blocking action on the cardiac ventricular Na^+ channels explains the well-known 'quinidine-like' side effect of neuroleptics (Ogata & Narahashi, 1989; Ogata *et al.*, 1989a). Furthermore, Cpz also exerted a potential blocking action on the different types of neuronal Ca^{2+} channels in a manner distinct from the action on the Na^+ channels (Narahashi *et al.*, 1989).

Recently, several investigators have succeeded in acutely dissociating the brain neurones from newborn or adult rodents and in recording voltage-gated as well as receptor-operated ionic currents from these neurones by use of the patch-clamp technique (Huguenard & Alger, 1986; Kay & Wong, 1986; Kaneda *et al.*, 1988). We have recently developed a technique to dissociate single striatal neurones from adult guinea-pig brain. This preparation allowed precise voltage- and space-clamp controls which are indispensable for accurate measurements of voltage-gated Na^+ currents. The aim of this study

was, therefore, to examine the effect of Cpz on the gating kinetics of the Na^+ channels in acutely dispersed striatal neurones of the guinea-pig.

Methods

Adult guinea-pigs of either sex (200 g) were decapitated, and the forebrain region was sliced in the sagittal direction (300 μm thick) according to the technique described elsewhere (Abe & Ogata, 1982). The technique for dispersion of the brain neurones was basically the same as the techniques described by others (Kay & Wong, 1986; Kaneda *et al.*, 1988). The caudate-putamen was dissected out under a binocular microscope (see Figure 1a) and incubated in a medium (36°C) of the following composition (in mM): NaCl 120, KCl 5, $CaCl_2$ 1.8, $MgCl_2$ 1, piperazine-N,N'-bis[2-ethanesulphonic acid]-Na (PIPES-Na) 5 mM and glucose 25 mM with 0.5% trypsin (Sigma) added. During the incubation, the slices were continuously bubbled with 100% O_2. After 1 h of incubation, the slices were gently agitated with a fire-polished Pasteur pipette (inner tip diameter, 100 μM).

Electrical recording

The methods for electrical recording used in the present study were similar to those described in a

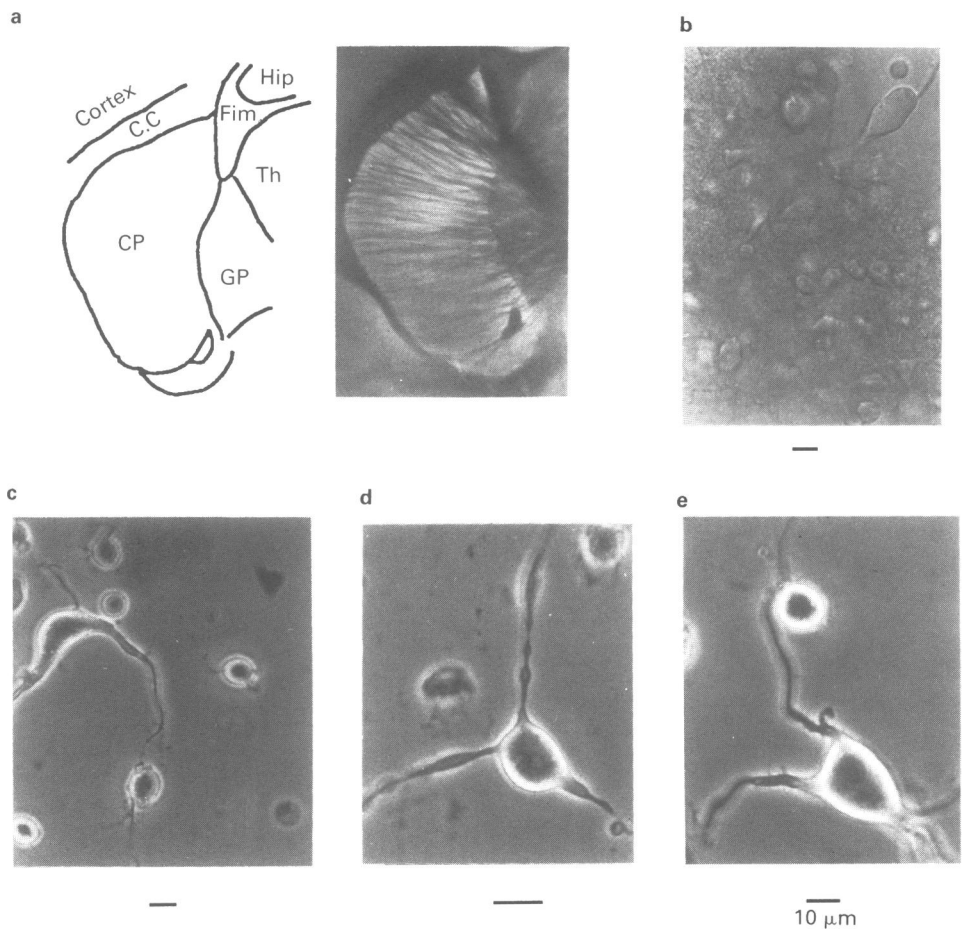

Figure 1 Striatal neurones of the adult guinea-pig. (a) Anatomical schema of the striatal region and a photograph of a striatal slice. C.C., corpus callosum; Fim, fimbria; Hip, hippocampus; CP, caudate putamen (striatum); GP, globus pallidum; Th, thalamus. (b) Nomarski interference microscopic observation of the tissue fragments produced by mild agitation. (c–e) Phase-contrast photomicrographs of typical examples of the freshly dissociated adult striatal neurones (see text, for explanation).

previous paper (Ogata & Narahashi, 1989). Briefly, a whole-cell variation of the patch-clamp technique (Hamill *et al.*, 1981) was used. Suction pipettes with a resistance of 1.2–2 MΩ were made of borosilicate glass capillary tubes using a 2-stage vertical puller and were fire polished. Inverted command pulses were applied to the bath through an Ag-AgCl pellet/3 M KCl agar bridge. The pipette potential was maintained at the ground level. Membrane currents passing through the pipette were recorded by a current-to-voltage convertor designed by M. Yoshii (Narahashi *et al.*, 1987) and stored digitally with a personal computer (PC-9801, NEC, Tokyo, Japan). Capacitative and leak currents were subtracted digitally by the P-P/4 procedure (Benzanilla & Armstrong, 1977). Fits to an exponential time course and a simple Boltzmann distribution were determined with the computer by a non-linear sum of the least squares fitting routine. The liquid junction potential between internal and external solutions recorded as zero current-potential was about −13 mV. The data shown here were compensated for this effect.

Solutions

The external and the internal (pipette-filling) solutions were designed to separate the Na^+ channel current (I_{Na}) from other voltage-dependent currents. The external solution contained (in mM): NaCl 100, tetraethylammonium (TEA)-Cl 25, $CaCl_2$ 1.8, CsCl 5, $MgCl_2$ 1, glucose 25, HEPES 5 and $CoCl_2$ 2. The solution was titrated to pH 7.4 with NaOH. The internal solution contained (in mM): Cs-glutamate 125, NaCl 10, $MgCl_2$ 2.5, HEPES 5, EGTA 5 and glucose 5. The pH of the internal solution was adjusted to 7.0 with CsOH. External TEA and replacement of external and internal K^+ with Cs^+ effectively suppressed the K^+ current, and external Co^{2+} totally suppressed the Ca^{2+} current. Cpz at a concentration of 10 mM was freshly prepared in each experiment and diluted to the desired concentration just before use. Unless otherwise specified, experiments were carried out at room temperature (22°C). Results are expressed as means ± s.e.mean. Significant differences from control were evaluated by Student's *t* test.

Results

The cells retained a good viability after enzymatic dissociation and stable Na^+ currents could be recorded. A nomarski interference microscopic observation of the tissue fragments produced by mild agitation provided a good estimate of the cellular composition within the tissue. As shown in Figure 1b, within the mildly agitated tissue fragment, individual cells were visible yet the cellular architecture of the tissue was preserved. Due to the thickness of the preparation, only a small percentage of the cells was in focus. However, in actual observations, a sharp outline of most of the cells could be observed by bringing them into focus.

The striatum of the adult guinea-pig contained two major morphological cell types depending on the shape and size of the soma as shown in Figure 1c. The overwhelming majority (greater than 95%) of the striatal neurones were of medium size (12–16 μm in diameter when measured across their greatest dimension) and had a round cell body with fine processes having poor arborization. A typical example of a medium-sized cell is shown in Figure 1d. Another 3–5% had polymorphic and large cell bodies (22–26 μm shortest dimension and 30–45 μm largest dimension). A typical example of a large cell is shown in Figure 1e together with a medium-sized round cell. These observations are consistent with histological data based on microscopic studies on the striatum (e.g., Lu & Brown, 1977; Chang *et al.*, 1982). Processes appeared to be thicker than their actual size, since most of the processes were out of focus due to their three-dimensional orientation. The medium-sized neurones were particularly advantageous for space-clamp control in the voltage-clamp experiment, and therefore, in the experiments described in this paper, we used only the medium-sized neurones.

Steady-state block of Na^+ current

Striatal neurones developed fast and transient inward currents. Since these currents were blocked by a low concentration of tetrodotoxin (0.1 μM), disappeared in Na^+-free solution and persisted during perfusion of inorganic Ca^{2+} blockers such as 2 mM Co^{2+}, it was concluded that these currents were carried by Na^+. Figure 2 shows I_{Na} recorded from a medium-sized striatal neurone and the effect of Cpz on this current. Figure 2a illustrates the experimental protocol used for subtraction of the capacitative and leak currents. The test pulse (V_p) was followed by 4 repetitive pulses whose amplitude was reduced to 1/4 of V_p and the polarity was reversed ($V_{-P/4}$). Each interval was 0.5 s. Since the leak conductance measured at a potential range of −150 to +50 mV was linear in our experimental situation in which internal and external K^+ were substituted by equimolar amounts of Cs^+, the summation of current traces generated by the above 5 consecutive pulses effectively subtracted both the capacitative and leak components from the test pulse current.

I_{Na} produced by a step depolarization to −10 mV was inhibited by Cpz 4 μM by about 50% (Figure 2b). The current trace obtained in the presence of Cpz

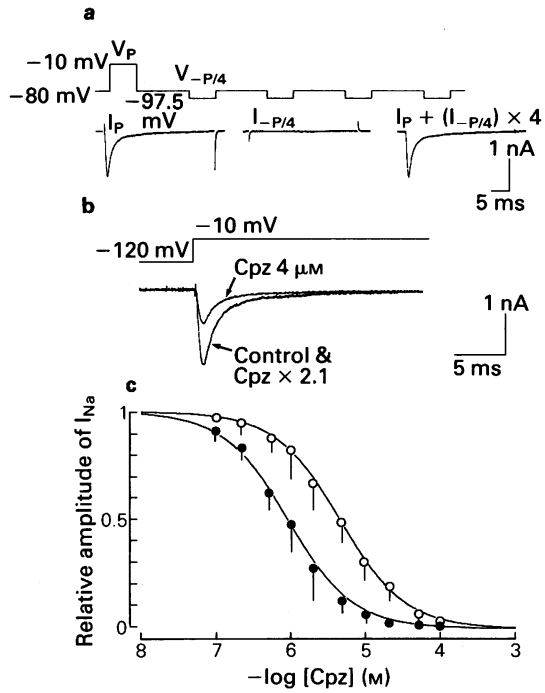

Figure 2 Effects of chlorpromazine (Cpz) on I_{Na} in the freshly isolated guinea-pig striatal neurone. (a) Illustrates a P-P/4 protocol used to eliminate capacitative and leak components from the current obtained in response to test pulses. (b) Illustrates the effect of Cpz on I_{Na} induced by a step depolarization to −10 mV. The current trace obtained in the presence of Cpz is scaled to the control current (Cpz × 2.1). (c) Concentration-response relationships after Cpz block of I_{Na}. The amplitudes of peak I_{Na} in the presence of Cpz elicited by 30 ms test pulses to −10 mV from a holding potential (V_h) of −120 mV (○) or −70 mV (●) were normalized to the control amplitude. Each point represents the mean from 5–7 experiments and vertical lines show s.e.mean. Curves were drawn according to the following equation:

$$I_{Na} = 1/(1 + [Cpz]/K_d)$$

where K_d is the dissociation constant of the binding reaction Cpz + X = CpzX. Here, X represents the channel in the unblocked configuration. In this and subsequent figures (except Figure 6), a P-P/4 protocol has been employed. Upward and downward deflections represent outward and inward currents, respectively.

was scaled to the control by multiplying the amplitude by 2.1. Both the activation and decaying phases completely overlapped with those of the control current in all 10 cells examined. The action of Cpz was usually apparent within 1 min after the drug was added, stabilized within 5 min or less, and full recovery occurred 5–10 min after washing. The blocking action of Cpz was not affected by lowering the medium temperature to 11°C.

Figure 2c shows the concentration-dependence of the blocking action of Cpz on I_{Na}. The peak amplitudes of I_{Na} in response to depolarizing test pulses to −10 mV were plotted as a function of Cpz concentration. When a holding potential (V_h) was −120 mV, the half-maximal inhibition of I_{Na} by Cpz occurred at 4.9 μM (open circles in Figure 2c). The lines in Figure 2c are theoretical curves corresponding to binding reactions where one Cpz molecule is necessary to block a single Na^+ channel. The concentration-dependence of the current amplitude was best fitted with 1 : 1 stoichiometry (theoretical curves for 2 : 1 and 3 : 1 which deviated from the measured curve were not illustrated for clarity). Thus, the cooperation of one Cpz molecule appears to be required to block a single Na^+ channel.

The concentration-response curve shifted to the left when the membrane was held at a more depolarized level (filled circles in Figure 2c). At a V_h of −70 mV, the half-blocking concentration was reduced from 4.9 μM to 0.9 μM. A one-to-one binding curve provided a good fit to the data as in the case of −120 mV V_h.

Figure 3 shows the effect of Cpz on the relationship between the depolarizing command potential and the peak amplitudes of I_{Na}. I_{Na} was activated at −50 mV, peaked at −20 mV and reversed its polarity at +60 mV. Cpz (5 μM) reduced the peak current amplitudes to 50.8 ± 4.6% ($n = 5$) of the control. There was no detectable voltage-dependence for the block, as shown in Figure 2c. The curve obtained by multiplying the values of the current-voltage curves in the presence of Cpz (open squares) by 1.85 times overlapped with the control current-voltage curve (open circles).

Effects of Cpz on activation kinetics

The instantaneous current upon repolarization (tail current) was measured to study the steady-state activation curve of I_{Na}. Figure 4a shows the tail currents upon clamp-back to a fixed potential (−80 mV) from −20 mV measured at various times following the appearance of I_{Na}. The steady-state activation (m_∞) curve is usually compiled from the tail current measured at a fixed time after the onset of step depolarization. However, as shown in Figure 3b, the time to the peak of I_{Na} changed depending on the magnitude of the step depolarization. Therefore, we measured the time-dependence of the tail current amplitude by changing the duration of step depolarization (see Figure 4a), and determined the maximum amplitude of the tail current at various levels of step depolarization.

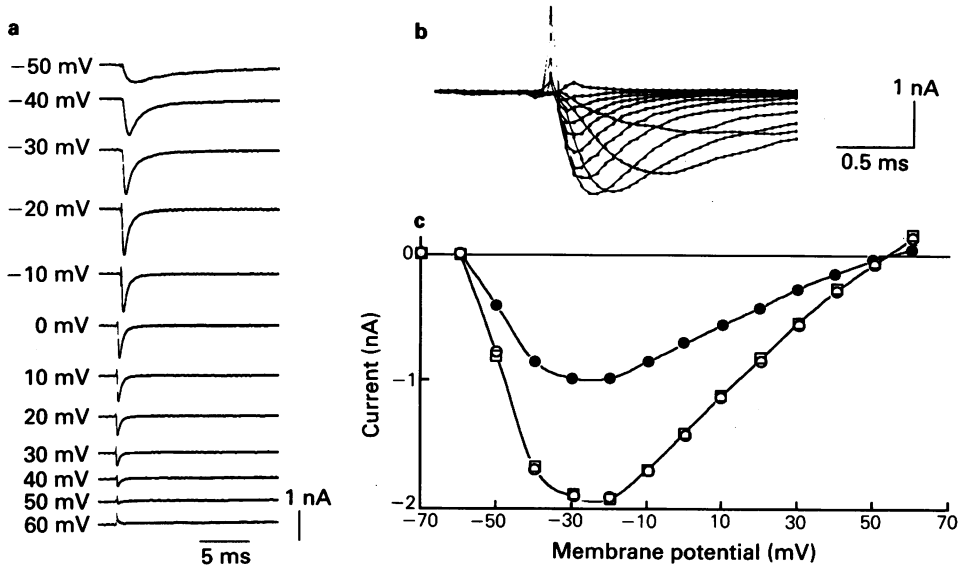

Figure 3 Effects of chlorpromazine (Cpz) on the current-voltage relationship for I_{Na}. (a) Shows a family of I_{Na} elicited by 20 ms step depolarizations to −50–+60 mV from V_h of −80 mV. Step depolarizations were applied at a constant rate of 0.03 Hz. The same recordings were shown superimposed in a faster time scale in (b). (c) The peak amplitudes of I_{Na} plotted as a function of test potentials, in controls and in the presence of Cpz; (○) control, (●) Cpz 5 μM and (□) Cpz × 1.85.

The time course I_{Na} can be described by:

$$\exp(-t/\tau_m) = 1 - [I(t)/I'(t)]^{1/n} \quad (1)$$

where τ_m is the time constant of activation kinetics, n is an integer, and I(t) and I'(t) represent the recorded current amplitude and the current amplitude estimated from the extrapolation of the decay phase of I_{Na} at time t (Ogata & Narahashi, 1989). The plot of values, $1 - [I(t)/I'(t)]^{1/n}$, on a semi-logarithmic scale against t should fall on a straight line if an appropriate value of n is given. As shown in Figure 4b, the plot fell on a straight line when n was 3, indicating that the activation process is best described by m^3 kinetics. τ_m measured at −30 mV was 0.16 ± 0.02 ms ($n = 4$). Cpz (2–5 μM) had no effect on the τ_m ($P > 0.05$, $n = 4$).

The m_∞ curves were made by calculating the cube root of the peak amplitude of the tail current (Figure 4c). The slope factor for e-fold change in the control m_∞ measured at the mid-point potential (−25.5 ± 2.0 mV, $n = 4$) was 11.7 ± 2.3 mV. Cpz (2.5 μM) had no effect on the m_∞ curves in any of 3 cells examined.

Steady-state inactivation

Since a membrane depolarization, which increases the proportion of the inactivated state of the channel, augmented the channel block by Cpz (Figure 2c), Cpz might preferentially bind to inactivated channels with higher affinity than to the resting channels and stabilize them in the inactivated state. We, therefore, tested this possibility by measuring the steady-state availability of Na^+ channels. Figure 5a shows an experimental protocol. Inactivation characteristics were studied by varying the conditioning potential ($V_{conditioning}$) and applying test pulses (V_{test}) to −10 mV. A plot of peak current amplitude against $V_{conditioning}$ gives a measure of the voltage-dependence of inactivation. To avoid distortion of the measurement by fluctuation of control I_{Na} during a course of recording, control I_{Na} ($V_{reference}$) was measured 10 s before each $V_{conditioning}$. The 10 s interval was sufficient for recovery from inactivation. Experiments in which the amplitude of control I_{Na} changed more than 10% were discarded. The steady-state inactivation (h_∞) was calculated by the ratio, $I_{test}/I_{reference}$.

The inactivation curve had a slope parameter (k) of 6.3 mV and a mid-point voltage ($V_{1/2}$) of −65 mV (Figure 5b). The h_∞ curve in the presence of Cpz (2.5 μM) revealed a parallel shift of about 12 mV (12.6 ± 3.8 mV, $n = 4$) toward a more negative potential, indicating that the blocking action of Cpz is voltage-dependent. The slope factor which reflects the voltage sensitivity of the inactivation gating was not affected by Cpz. The actual size of I_{Na} available

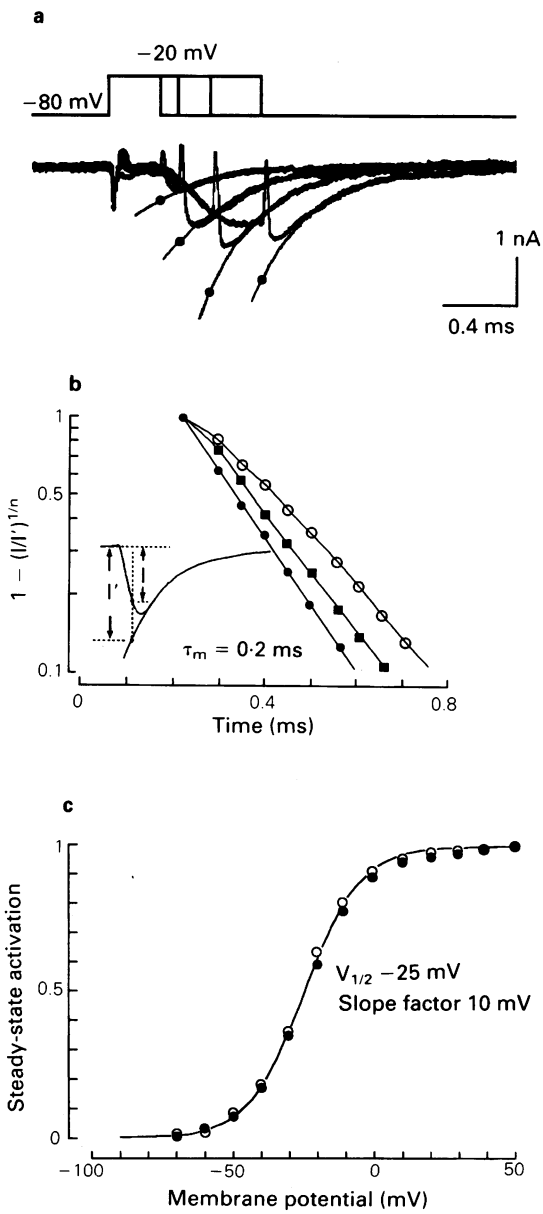

Figure 4 The steady-state activation (m∞) curves for I_{Na} in the presence and absence of chlorpromazine (Cpz). (a) Tail currents measured after the depolarizing command potentials of various duration. The membrane was depolarized to −20 mV from V_h of −80 mV for a period of ΔT. The initial portion of the tail current was obscured due to the P-P/4 procedure. However, this did not affect the exponential fitting of the decaying phase of the tail current. The deactivation time course of the tail current was expressed by a single exponential function (solid lines). The dots on the solid lines represent the initial amplitude of the tail current determined by extrapolating the falling phase to the time of repolarization. (b) The time course of I_{Na} activation was assessed by equation (1) described in the text. I and I' represent the recorded current amplitude and the current amplitude estimated by the extrapolation of the decay phase, fitted by a single exponential function for test potential of −30 mV from a V_h of −80 mV (see inset). The value, $1 - [I(t)/I'(t)]^{1/n}$, was plotted against time on a semi-logarithmic scale. (○) $n = 1$, (■) $n = 2$, (●) $n = 3$. (c) The cube root of the maximal amplitude of the tail current was plotted as a function of the levels of step depolarization. The smooth curves were drawn according to the equation:

$$m\infty = 1/(1 + \exp[-(V_{test} - V_{1/2})/\kappa])$$

where V_{test} is the potential level of the step depolarization and $V_{1/2}$ is the V_{test} where I_{Na} is one-half maximal, and κ is the slope factor (10 mV). (○) Control, (●) in the presence of Cpz 2.5 μM.

at very negative conditioning potentials (−100 to −130 mV) decreased by about 32% (see the curve drawn by dotted line). This decrease was equivalent to that expected from the concentration-response curve (Figure 2c).

Dissociation constant for binding of Cpz to the inactivated Na^+ channels

The binding of Cpz to the inactivated Na^+ channel is electrically silent, since the channels are already non-conducting and not available for opening. It is, therefore, impossible to measure directly K_i, the dissociation constant for the binding of Cpz to the inactivated Na^+ channels. We estimated it using several equations. There is a relationship between K_i, K_{rest} and $K_{apparent}$ (the dissociation constant that is determined by a mix of the actual binding reactions to resting and inactivated channels) described by (Bean *et al.*, 1983; Bean, 1984):

$$K_{apparent} = 1/[h\infty/K_{rest} + (1 - h\infty)/K_i]$$

The h∞ at V_h of −70 mV was 0.77 (Figure 5) and K_{rest} and $K_{apparent}$ were 4.9 and 0.9 μM, respectively (Figure 2c). Therefore, calculated K_i was 0.24 μM.

The K_i can also be deduced from the voltage-dependence of I_{Na} availability (Bean *et al.*, 1983). The shift in midpoint of the h∞ curve in the presence of Cpz, ΔV (−15 mV, Figure 5), is expressed, assuming one-to-one binding (Figure 3c), as:

$$\Delta V = k \ln\{(1 + [Cpz]/K_{rest})/(1 + [Cpz]/k_i)\}$$

in which k is the slope factor of the h∞ curve (6.3 mV, Figure 5) and [Cpz] is the concentration of Cpz. The calculated value of K_i was 0.14 μM, approximately the value estimated from the concentration-response curve (0.24 μM).

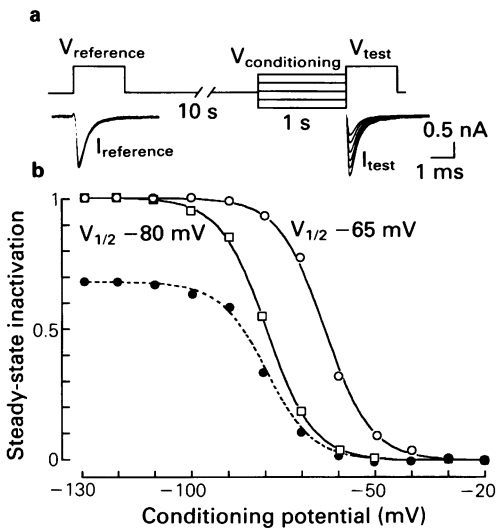

Figure 5 Steady-state inactivation ($h\infty$) curves for I_{Na} in the presence and absence of chlorpromazine (Cpz). (a) Experimental protocol. Two identical step depolarizations to −10 mV for 30 ms were applied 10 s before ($V_{reference}$) and immediately subsequent (V_{test}) to the conditioning pulse ($V_{conditioning}$). The potential level of $V_{conditioning}$ was changed from −130 mV to −20 mV in 10 mV steps. (b) The peak current amplitude measured during V_{test} was normalized to the control amplitude measured during $V_{reference}$ and plotted as a function of $V_{conditioning}$. The smooth curves were drawn according to the equation:

$$h\infty = 1/1 + \exp[(V_{conditioning} - V_{1/2})/\kappa])$$

where $V_{1/2}$ is the conditioning potential when I_{Na} is one-half maximal, and κ is the slope factor (6.3 mV). The curve indicated by (●) is drawn by multiplying the $h\infty$ in the presence of Cpz by 0.68, the reduction of I_{Na} at −120 mV by Cpz. (○) Control, (□) Cpz 2.5 μM.

Use-dependent block

In addition to the steady-state channel block, Cpz produced block of Na^+ channels during repetitive stimulation. Figure 6a shows the time courses of I_{Na} elicited by a train of depolarizing pulses. Eight consecutive pulses to −10 mV (30 ms duration) were applied from a V_h of −120 mV with various pulse intervals. The peak current amplitude for each pulse in the train was normalized to that of the first pulse and plotted against the pulse number. In control experiments (circles), the amplitude of I_{Na} remained constant at a pulse interval of 100 ms, indicating that normal Na^+ channels fully recover from inactivation within 100 ms after repolarization to −120 mV. In the presence of Cpz, a marked cumulative decrease of I_{Na} was seen in a wide range of pulse intervals

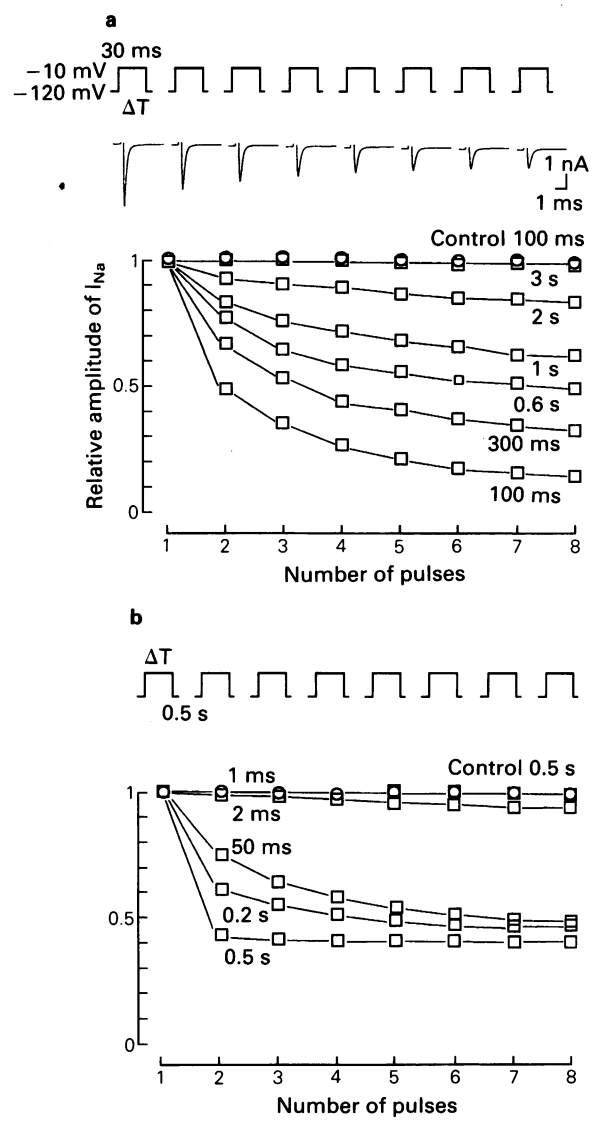

Figure 6 Time course of I_{Na} elicited by a train of step depolarizations applied at various pulse intervals. (a) Eight consecutive pulses to −10 mV (30 ms duration) were applied from a V_h of −120 mV at various pulse intervals ranging from 100 ms to 3 s. Inset: current traces in response to repetitive step depolarizations applied with 300 ms intervals in the presence of chlorpromazine (Cpz, 2.5 μM). The peak current amplitude for each pulse in the train was normalized to that of the first pulse and plotted against the pulse number. (○) Control; (□) in the presence of Cpz (2.5 μM). Numerals attached to the traces indicate interpulse intervals of repetitive stimulation. (b) Eight consecutive pulses to −10 mV (duration, 1–500 ms) were applied from a V_h of −120 mV with a fixed interval (500 ms). (○) Control; (□) in the presence of Cpz (2.5 μM).

from 100 ms to 2 s. Hereafter, this type of block seen during repetitive pulsing will be referred to as 'use-dependent block'. An interval of 3 s was required to avoid use-dependent block of I_{Na}. Similar results were obtained in all 8 cells examined.

Figure 6b shows an experiment similar to that in Figure 6a, but here, the protocol was designed to assess the time-dependence of the blocking process. The pulse duration was variable and the pulse interval was fixed at 500 ms. An interval of 500 ms was long enough to allow the normal channels to recover from inactivation but short enough for the drug-bound channels to reprime (as shown later). In the control experiments, I_{Na} remained constant in all the cases where the pulse duration was 50, 200 or 500 ms (only the plots for 500 ms are illustrated for clarity). In the presence of Cpz, the use-dependent block was not produced when pulse duration was 1 ms in any of the 3 cells examined. However, lengthening of the pulse duration to longer than 50 ms produced a marked use-dependent block. When the pulse interval was 50 or 200 ms, I_{Na} was progressively reduced during repetitive depolarization. When the pulse interval was increased to 500 ms, the second I_{Na} reached a steady-state value.

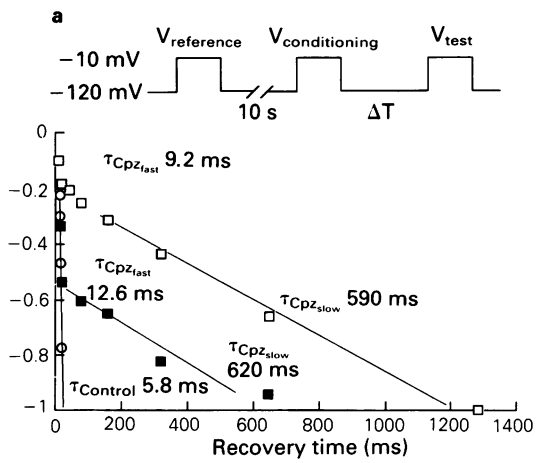

Figure 7 Dissociation of chlorpromazine (Cpz) from the inactivated Na^+ channel. (a) Recovery from inactivation was assessed using a double pulse protocol shown in the inset. A conditioning pulse to −10 mV ($V_{conditioning}$) was followed by a variable recovery period, and then by a test pulse to −10 mV (V_{test}) for 30 ms. Each two-pulse sequence was given at 30 s intervals. The peak amplitude of the test current was normalized to that of the preceding control current evoked by $V_{reference}$ and $\log(1 - I_{test}/I_{reference})$ was plotted as a function of the recovery period (ΔT). (○) Control; in the presence of Cpz 1 μM (■) or 2.5 μM (□). (b) Illustrates the currents evoked by $V_{reference}$ and V_{test} in the presence of 2.5 μM Cpz (the periods of $V_{conditioning}$ and ΔT were not sampled).

Kinetics of the use-dependent block

The results so far obtained suggest that Cpz preferentially binds to the Na^+ channel in its inactivated state and stabilizes it. Therefore, recovery from inactivation is expected to be delayed in the presence of Cpz. This was examined by use of a double-pulse protocol (Figure 7). A 500 ms conditioning pulse to

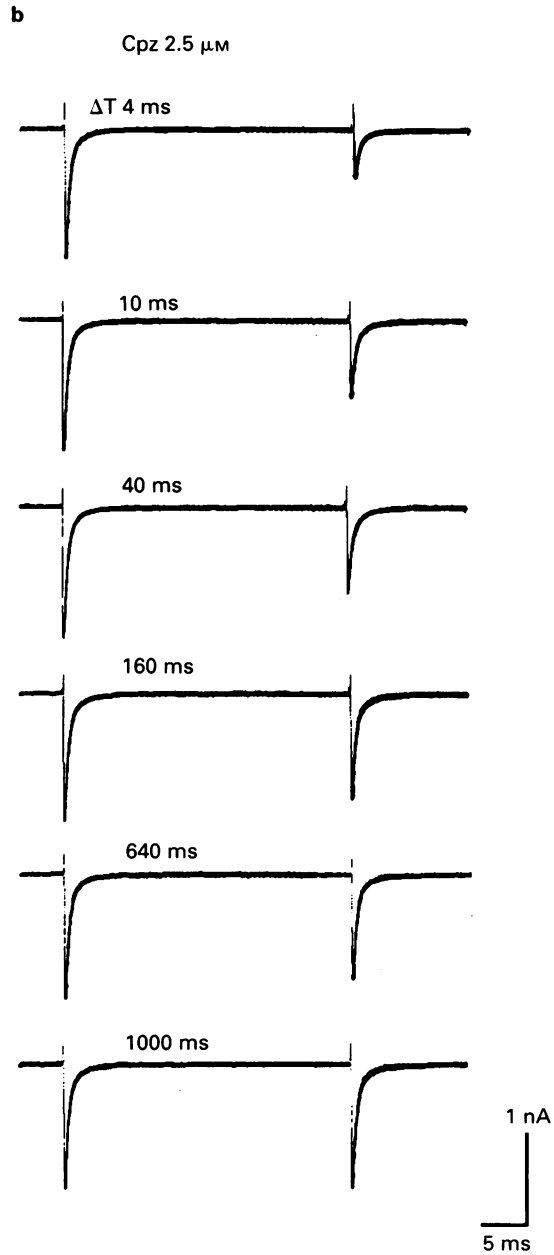

−10 mV was followed by a variable recovery period, and then by a test pulse to the same potential. The duration of the conditioning pulse of 500 ms was sufficient to produce maximal steady-state block (see Figure 6b). Each set of two pulses was given at an interval of 30 s. The peak current for each test pulse (V_{test}) was normalized to that for the preceding control pulse ($V_{reference}$) and plotted as a function of the recovery period (ΔT).

The test currents in the drug-free solution completely recovered within 20 ms with a time constant of 5.6 ± 0.6 ms ($n = 5$) (open circles). In the presence of Cpz (2.5 μM), the time course of recovery was markedly slowed, and a recovery period longer than 1 s was necessary to obtain full recovery (open squares). The recovery time course was characterized by two exponentials. The time constants of recovery were 8.9 ± 0.7 ms and 602 ± 64 ms ($n = 5$) for the fast and slow components, respectively. The fast time constant approximated the time constant of the control. Lowering the Cpz concentration to 1 μM resulted in a reduction of the amplitude of the slow component (filled squares). Figure 7b illustrates the $I_{reference}$ and I_{test} recorded at various recovery periods (ΔT).

Figure 8 illustrates how Na^+ channel inactivation was accelerated by Cpz during maintained membrane depolarization. As shown in the inset of Figure 8, a test pulse to −10 mV was preceded by a conditioning pulse to −10 mV with various durations. An interpulse-interval of 500 ms was put between the conditioning and test pulses to allow drug-unbound normal channels to reprime fully from the inactivated state to the resting state (see Figure 6b in which a test pulse of 500 ms duration had no effect on the Na^+ current evoked by subsequent test pulses in the control medium). The peak amplitude of the test current was normalized to that of the reference current measured 10 s before the conditioning pulse, and plotted against the conditioning pulse duration (ΔT) on a normal (upper half) and semi-logarithmic (lower half) scale. The Na^+ current in the presence of Cpz decreased to a steady-state level with a two exponential time course (τ_{fast}, 16.0 ± 1.8 ms; τ_{slow}, 162.5 ± 13.8 ms).

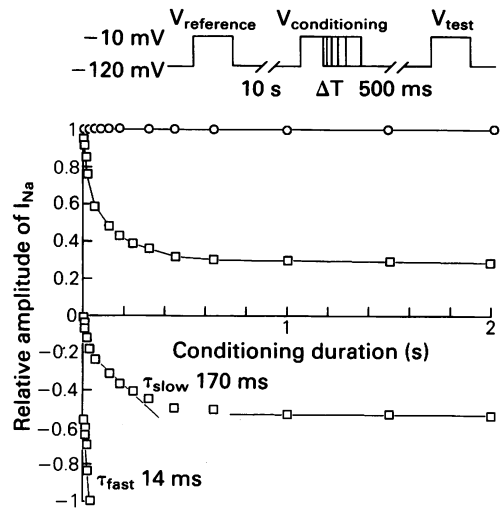

Figure 8 Association of chlorpromazine (Cpz) to the inactivated Na^+ channel. Inset shows an experimental protocol. A conditioning pulse ($V_{conditioning}$) to −10 mV of varying duration was followed by a 500 ms recovery period and then by a test pulse (V_{test}) of 30 ms duration. An identical pulse to V_{test} was applied 10 s before the conditioning pulse ($V_{reference}$). The peak amplitudes of test currents were normalized to those of control I_{Na} evoked by $V_{reference}$, and plotted against the conditioning duration on a normal (upper half) or semi-logarithmic scale (lower half). The lines were drawn by eye. (○) Control; (□) in the presence of Cpz (2.5 μM).

Discussion

The present study shows that the Na^+ channel gating kinetics are retained after enzymatic dissociation of the cells in the mammalian brain. The use of small (12–16 μm) neurones that have relatively fine processes (Figure 1) contributed to the quality of voltage-clamp control, as evidenced by a gradual increase of peak I_{Na} in the negative slope region of the I–V curve without 'threshold phenomenon' (Figure 3b), a single exponential decay of the tail currents (Figure 4a), and a consistent peak-latency of I_{Na} during multiple changes of the current amplitude (Figure 5a).

Interaction of Cpz with resting Na^+ channels

Our data indicate that Cpz has a potent blocking action on I_{Na} of the guinea-pig striatal neurones. Since the block was seen at a low temperature (11°C), this action appears to be due to a direct action on the ion channel rather than to some indirect effect. We have shown that the block of I_{Na} in the guinea-pig ventricular myocytes was the result of a direct action on the ion channel (Ogata *et al.*, 1989a). In this respect, Benishin *et al.* (1988) demonstrated that the inhibition of the calcium-activated K^+ channel in rat forebrain synaptosomes by neuroleptics is not mediated by calmodulin.

It appears that the blocking action of Cpz can be interpreted on the basis of the modulated receptor hypothesis introduced for local anaesthetic block of Na^+ channels (Hille, 1977; Hondeghem & Katzung, 1977). At very negative (−120 mV) V_h, where most

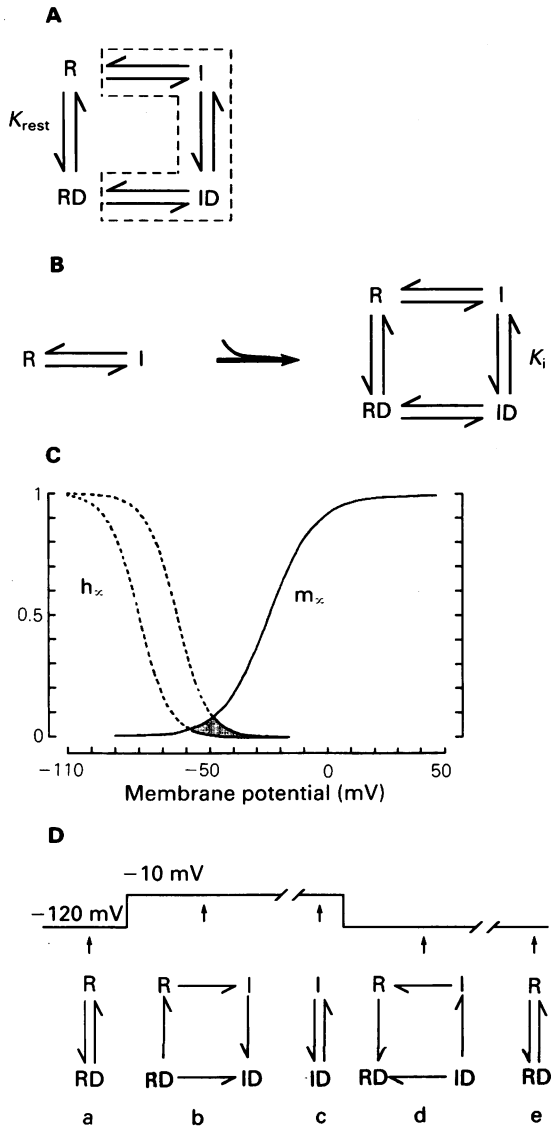

Figure 9 Modulated-receptor model for chlorpromazine (Cpz) binding. The size of the symbols indicating the channel state represent the relative population of the channel at that state. The scheme ignores interactions between Cpz and the open state of the channel, since our data suggested that these are negligible for interpretation of our experimental results. It should be noted that the illustrations are given for the sake of intuitive explanation and do not provide a correct picture of the channel states. (A) Illustrates the channel state at a very negative V_h in the presence of Cpz to explain resting block. The channel states enclosed by the broken line indicate that the channel population is negligibly small or absent. (B) Illustrates the shift of h_∞ curve by Cpz. The m_∞ and h_∞ curves shown in Figures 7 and 8 are drawn together in (C) to indicate a decreased 'window current' (shaded area) by Cpz. (D) The channel states at a very negative V_h (a), during a prolonged membrane depolarization (b and c), and after clamp-back to the initial V_h (d and e) to explain the association and dissociation of Cpz with the inactivated channel. R, resting state; RD, resting state with Cpz bound; I and ID, corresponding forms of the inactivated state; K_{rest} and K_i, the dissociation constants for resting and inactivated channels, respectively.

of the channels are in a resting state, i.e., ready to open upon depolarization ($h_\infty = 1$), (see Figure 5b), Cpz reduced the amplitude of I_{Na} (Figure 2b). This block is, therefore, thought to be due to the binding of Cpz to the resting channels (Figure 9A). The dissociation constant for this binding (K_{rest}) can be obtained from the concentration-response curve measured at a V_h of -120 mV (4.9 μM, see Figure 2c).

Interaction of Cpz with open Na^+ channels

I_{Na} in the presence of Cpz overlapped with control I_{Na} when the peak amplitude was normalized to the control (Figure 2b), indicating that Cpz does not affect τ_m or τ_h, the rates at which Na^+ conductance approaches its maximum or declines to its minimum. The above observation also suggests that Cpz does not interact with the open configuration of the channel (Colquhoun & Hawkes, 1983; Lee & Tsien, 1983). This idea is strengthened by a lack of voltage-dependence of the I–V curve (Figure 3c). Further supporting evidence was provided by the observation that, in the presence of Cpz, the use-dependent block was not produced when repetitive pulses to -10 mV were delivered with a pulse duration of 1 ms (Figure 6b). Since τ_m at a membrane potential of -10 mV was smaller than τ_m at -30 mV (0.2 ms, see Figure 4b) and τ_h was 1.6 ms (calculated from the trace in Figure 2b), a step depolarization to -10 mV for 1 ms is long enough to initiate the activation but too short to produce an appreciable amount of inactivation. Therefore, if Cpz interacted with the open Na^+ channel, I_{Na} should have become smaller during repetitive pulses due to the use-dependent (current-dependent) block.

Interaction of Cpz with inactivated Na^+ channels

Due to the shift in the h_∞ curve toward a more negative potential (Figure 5b), the action of Cpz is markedly enhanced under conditions where the membrane is depolarized. The dissociation constant for the binding to the inactivated state of Na^+ channels, K_i, (0.24 or 0.14 μM) appears to be 20–30 times smaller than K_{rest} (4.9 μM) and below the clinical concentration of this drug (Cooper *et al.*, 1976). Therefore, the action of Cpz may become significant in

pathological conditions in which the membrane is depolarized.

One possible explanation for the shift of the $h\infty$ curve is the change in the gating kinetics of the channel. Since $h\infty$ is described by $\alpha_h/(\alpha_h + \beta_h)$, where α_h and β_h are the rate constants for channel opening and closing, the reduction of $h\infty$ could be attributed to a change in the ratio, β_h/α_h. However, the observation that the decay time constant of I_{Na} which can be expressed by $1/(\alpha_h + \beta_h)$ was not affected by Cpz does not favour this idea.

The shift in $h\infty$ might be best explained by an increased population of the quiescent channels due to a production of drug-bound inactivated channels. As illustrated in Figure 9B, channels are distributed to R and I at depolarized membrane potentials in the control solution. Application of Cpz causes binding of Cpz to R and I with K_{rest} and K_i. Since $K_{rest} \gg K_i$ (see below), $I \rightarrow ID$ is much greater than $R \rightarrow RD$. The overwhelming binding of Cpz to I causes a proportional decrease in R due to the equilibrium between resting and inactivated channels, thus reducing $h\infty$.

As shown in Figure 9C, there was a significant degree of overlap between the inactivation and activation curves in the control solution, suggesting that Na^+ channels of the guinea-pig striatal neurones may be capable of supporting a steady influx of Na^+ (window current) over a narrow range of potentials. Application of Cpz which shifted the $h\infty$ curve to the left (Figure 5b) without affecting the $m\infty$ curve (Figure 4) cancels most of the window current (shaded area in Figure 9C). This effect of Cpz might be significant in the regulation of steady-state excitability of the neurone.

Kinetics of the use-dependent block

As was observed in the guinea-pig ventricular myocyte (Ogata & Narahashi, 1989; Ogata *et al.*, 1989a), the action of Cpz was promoted by repetitive activation of the channel (Figure 6). This use-dependent effect appears to be due to the slow re-priming of the Cpz-bound channels, since the block of open-channels did not appear to play a dominant role, at least in the concentrations we used (see above). As shown in Figure 7, recovery from inactivation was expressed as two exponentials. Since the fast component had a time course comparable to that of the recovery of the normal Na^+ channels, this may reflect the recovery of the unbound channel fraction (I in Figure 9D, c). Alternately the slow component might represent the recovery of the drug-bound channel fraction which was temporally produced during a conditioning depolarization (ID in Figure 9D, c). The dissociation of Cpz from the inactivated channels is shown schematically in Figure 9D ($c \rightarrow d \rightarrow e$) in terms of the change of the channel equilibrium states.

When the duration of the test pulse was 30 ms, the use-dependent block did not attain a steady-state value during eight consecutive test pulses (Figure 6a). Since the use-dependent block reflects the successive decrease of the channel populations, R + RD in Figure 9D, a, the above observation might indicate that the 30 ms duration was too short to reach an equilibrium between I and ID (Figure 9D, c). The experiment in Figure 6b measures the time-dependence of this equilibration. If the test pulse duration is long enough to allow the channels to be redistributed to I and ID in equilibrium (from a to c in Figure 9D), the amplitudes of I_{Na}s evoked by test pulses subsequent to the first test pulse should become constant, with their absolute values determined by the interpulse interval. Thus, it appears that the shift of the channel population from 'a' to 'c' in Figure 9D takes more than 200 ms.

The question is what is the pathway of the movement of RD to ID and which portion of the pathway is rate-limiting. An experimental approach to this question is shown in Figure 8. The time course of I_{Na} in this figure reflects the time constant of the association of Cpz with the inactivated Na^+ channels, because during a 500 ms interpulse interval, normal Na^+ channels are fully reprimed (see Figure 7a). The time course of I_{Na} was expressed as:

$$I_{Na}(t) = 0.33 + 0.28 \exp(-t/\tau_{fast}) + 0.39 \exp(-t/\tau_{slow}),$$

where τ_{fast} and τ_{slow} are 14 ms and 170 ms, respectively. The first term is the steady-state value of the use-dependent block. In other words, it reflects the amount of R in Figure 9D, d. The two time constants represent the rates by which the state 'a' shifts to 'c' in Figure 9D. The channel fraction R moves to ID via $R \rightarrow I \rightarrow ID$. The time required for the shift of the channel from R to I is estimated from the values of τ_m and τ_h and is thus negligible (in the order of 1 or 2 ms). The pathway from I to ID does not appear to be the rate-limiting step of the slow use-dependent effect, since repetitive pulse of 30 ms duration produced an appreciable amount of use-dependent block (Figure 6a). If we assume that RD directly moves to ID, its time course will be described by a single exponential function. If RD moves to ID via R and I, its time course will be expressed by a multi-exponential function. Taken together, the most likely explanation for the above two exponential time courses might be that the fast component mainly reflects the process, $I \rightarrow ID$ and the second com-

ponent represent the process, RD → R or RD → ID. The prolonged time course of the use-dependent block thus appears to be due to the slow kinetics of the drug-bound Na^+ channels.

We are grateful to Prof. H. Kuriyama for pertinent advice and criticism and to Dr M. Yoshii for providing on-line data processing program. This study was supported by the Japanese Ministry of Education (Scientific Research 63570096).

References

ABE, H. & OGATA, N. (1982). Ionic mechanism for the osmotically induced depolarization in neurones of the guinea-pig supraoptic nucleus *in vitro*. *J. Physiol.*, **327**, 157–171.

BEAN, B.P. (1984). Nitrendipine block of cardiac calcium channels: High-affinity binding to the inactivated state. *Proc. Natl. Acad. Sci. U.S.A.*, **81**, 6388–6392.

BEAN, B.P., COHEN, C.J. & TSIEN, R.W. (1983). Lidocaine block of cardiac sodium channels. *J. Gen. Physiol.*, **81**, 613–642.

BENISHIN, C.G., KRUEGER, B.K. & BRAUSTEIN, M.P. (1988). Phenothiazines and haloperidol block Ca-activated K channels in rat forebrain synaptosomes. *Molec. Pharmacol.*, **33**, 195–201.

BEZANILLA, F. & ARMSTRONG, C. (1977). Inactivation of the sodium channel I. Sodium current experiments. *J. Gen. Physiol.*, **70**, 549–566.

CHANG, H.T., WILSON, C.J. & KITAI, S.T. (1982). A Golgi study of rat neostriatal neurons: Light microscopic analysis. *J. Comp. Neurol.*, **208**, 107–126.

COLQUHOUN, D. & HAWKES, A.G. (1983). The principles of the stochastic interpretation of ion-channel mechanisms. In *Single Channel Recording*, ed. Sakmann, B. & Neher, E., pp. 135–175. New York: Plenum Press.

COOPER, T.B., SIMPSON, G.M. & LEE, H.J. (1976). Thymoleptic and neuroleptic drug plasma levels in psychiatry: current status. *Int. Rev. Neurobiol.*, **19**, 269–309.

HAMILL, O.P., MARTY, A., NEHER, E., SAKMANN, B. & SIGWORTH, F.J. (1981). Improved patch-clamp techniques for high resolution current recording from cells and cell-free membrane patches. *Pflügers Arch.*, **391**, 85–100.

HILLE, B. (1977). Local anesthetics: Hydrophilic and hydrophobic pathways for the drug-receptor reaction. *J. Gen. Physiol.*, **69**, 497–515.

HONDEGHEM, L.M. & KATZUNG, B.G. (1977). Time- and voltage-dependent interactions of antiarrhythmic drugs with cardiac sodium channels. *Biochim. Biophys. Acta*, **472**, 373–398.

HUGUENARD, J.R. & ALGER, B.E. (1986). Whole-cell voltage-clamp study of the fading of GABA-activated currents in acutely dissociated hippocampal neurons. *J. Neurophysiol.*, **56**, 1–18.

KANEDA, M., NAKAMURA, H. & AKAIKE, N. (1988). Mechanical and enzymatic isolation of mammalian CNS neurons. *Neurosci. Res.*, **5**, 299–315.

KAY, A.R. & WONG, R.K.S. (1986). Isolation of neurons suitable for patch-clamping from adult mammalian central nervous systems. *J. Neurosci. Methods*, **16**, 227–238.

LEE, K.S. & TSIEN, R.W. (1983). Mechanism of calcium channel blockade by verapamil, D600, diltiazem and nitrendipine in single dialysed heart cells. *Nature*, **302**, 790–794.

LU, E.J. & BROWN, W.J. (1977). The developing caudate nucleus in the euthyroid hypothyroid rat. *J. Comp. Neurol.*, **171**, 261–284.

NARAHASHI, T. (1974). Chemicals as tools in the study of excitable membranes. *Physiol. Rev.*, **54**, 813–889.

NARAHASHI, T., OGATA, N. & YOSHII, M. (1989). Differential block of sodium and calcium channels by chlorpromazine in mouse neuroblastoma cells. *J. Physiol.*, (in press).

NARAHASHI, T., TSUNOO, A. & YOSHII, M. (1987). Characterization of two types of calcium channels in mouse neuroblastoma cells. *J. Physiol.*, **383**, 231–249.

OGATA, N. & NARAHASHI, T. (1989). Block of sodium channels by psychotropic drugs in single guinea pig cardiac myocytes. *Br. J. Pharmacol.*, **97**, 905–913.

OGATA, N., NISHIMURA, M. & NARAHASHI, T. (1989a). Kinetics of blocking action of psychotropic drugs on sodium channels in single guinea pig ventricular myocytes. *J. Pharmacol. Exp. Ther.*, **248**, 605–613.

OGATA, N., YOSHII, M. & NARAHASHI, T. (1989b). Psychotropic drugs block voltage-gated ion channels in neuroblastoma cells. *Brain Res.*, **476**, 140–144.

(Received May 30, 1989
Revised July 12, 1989
Accepted August 3, 1989)